PAPER

Molecular dynamic simulation on temperature evolution of SiC under directional microwave radiation

To cite this article: Tahsin Ashraf Khan *et al* 2022 *J. Phys.: Condens. Matter* **34** 195701

View the article online for updates and enhancements.

Molecular dynamic simulation on temperature evolution of SiC under directional microwave radiation

Tahsin Ashraf Khan[1,*], [ID], **Patrick A Burr**[2] [ID], **David Payne**[1], **Mattias Juhl**[1], **Utshash Das**[1], **Brett Hallam**[3], **Darren Bagnall**[1] and **Binesh Puthen Veettil**[1]

[1] School of Engineering, Macquarie University, NSW 2109, Australia
[2] School of Material Science and Engineering, University of New South Wales, NSW 2207, Australia
[3] School of Photovoltaic and Renewable Energy Engineering, University of New South Wales, NSW 2207, Australia

E-mail: tahsin-ashraf.khan@students.mq.edu.au

CrossMark

Abstract
Silicon carbide (SiC) is widely used as the substrate for high power electronic devices as well as susceptors for microwave (MW) heating. The dynamics of microwave interaction with SiC is not fully understood, especially at the material boundaries. In this paper, we used the molecular dynamics simulation method to study the temperature evolution during the microwave absorption of SiC under various amplitudes and frequencies of the microwave electric field. Directional MW heating of a SiC crystal slab bounded by surfaces along [100] crystallographic direction shows significantly faster melting when the field is applied parallel to the surface compared to when applied perpendicular.

(Some figures may appear in colour only in the online journal)

1. Introduction

Microwave heating of materials has emerged as a fascinating research area during the past decade. El Khaled *et al* (7) showed in their work that energy exchange between microwaves and materials could be used as a viable alternative to conventional heating in some industries for thermal processing, owing to its better temperature control, volumetric, selective, and rapid heating. Although microwave heating and microwave annealing (MWA) techniques have been used in food industries as shown in the works of Ibrahim *et al* (11), and in ceramics and rubber industries mentioned by Singh *et al* (21), they are relatively new to semiconductor processing. Alford *et al* (2) has used MWA in semiconductor and photovoltaic industries to form shallow, well-defined p–n junc-

tions in ion-implanted silicon samples. Sarswat and Free (20) used microwave-based synthesis of CZTS (copper zinc tin sulphide) materials for photovoltaic applications in the field of semiconductors. Studying MWA and obtaining consistency in results has been challenging because the heating rates depend on numerous parameters such as moisture content, changes in dielectric properties with temperature, sample size, geometry, and the strength of the electric field, as mentioned in El Khaled *et al* (7) paper. The discrepancies in temperature measurements of the volumetrically heated samples have often resulted in reporting 'non-thermal' effects of microwave heating until it was disproven recently by the brilliant work of García-Baños et al (8).

Silicon carbide (SiC) assisted heating has been employed widely in the MWA applications for semiconductor processing demonstrated in the works of Kremsner and Kappe (15), Isfort *et al* (12) and many others. With the advent of high power and high-frequency electronics, the use of SiC as the

* Author to whom any correspondence should be addressed.

semiconductor substrate has been increasing, as pointed out in the works of Deng et al (6) and Nelson et al (17), thanks to its high power density, heat dissipation and bandwidth capability. Microwave absorption and heating in these substrate surfaces mainly depend on conductivity loss and polarisation relaxation loss as demonstrated in SiC nanotubes Gong et al (9), Zhang et al (29). The polarization loss seemed to be caused by the surface suspension bonds induced band gap reduction as observed by Yang *et al* (28), which is again observed in SiC nanowires by Jia et al (13).

Wang *et al* (25), Yang *et al* (27) and Liang *et al* (16) showed that SiC has also found widespread use as a susceptor material that enables secondary heating by microwave in ceramic, rubber, food and recycling industries. In both high-frequency switching applications and microwave processing applications, SiC absorbs microwaves through its intrinsic electric dipole polarization. Microwave absorption invariably results in substrate heating as seen by Cao et al (5), which is a desirable condition for microwave processing. As reported by Zhang et al (29) the real part of the permittivity has a direct proportionality with temperature, which is attributed to the shortened relaxation time of electron polarization. On the other hand, the imaginary part also increases which is ascribed to the increasing electrical conductivity of the carbon fibers in the carbon fibre/silica composite. Cao et al (4) and Jiang et al (14) experimentally demonstrated that the microwave absorption properties can be further altered by surface modification of the susceptor. However, a theoretical model for the heating dynamics of SiC with surface boundaries interacting with polarized microwave radiation is not yet reported.

Previous theoretical studies, such as WanJun *et al* (26) on SiC melting, were limited to perfect crystal structures with periodic boundary conditions and devoid of surfaces or defects. The experimentally observed variation or the jump in the heating rates of SiC for specific input MW field strengths showed by Tandon *et al* (22) could not be explained by those models. In this paper, the heating dynamics of bulk and slab SiC under polarized microwave radiation are studied using molecular dynamics (MD) simulations. The heating dynamics of SiC under polarized radiation applied perpendicular and parallel to the surface planes are also investigated.

2. Model and simulation details

Classical MD has been an effective tool for mathematically modelling and simulating material interactions at the molecular level, as presented by Brooks III et al (3). We used Large-scale Atomic/Molecular Massively Parallel Simulator (LAMMPS) software (30) to perform MD simulations for this work.

Atomic interactions were described based on the interaction potential introduced by Vashishta *et al* (23), which includes three-body interactions (necessary to model the partly covalent bonding of SiC) and Coulomb forces (required to account for microwave–matter interactions). Vashishta *et al* (23) mentions the charge transfer between Si and C atoms, resulting in the Coulomb interaction between ions. This calculation of Coulomb interaction is vital to include MW induced dipole
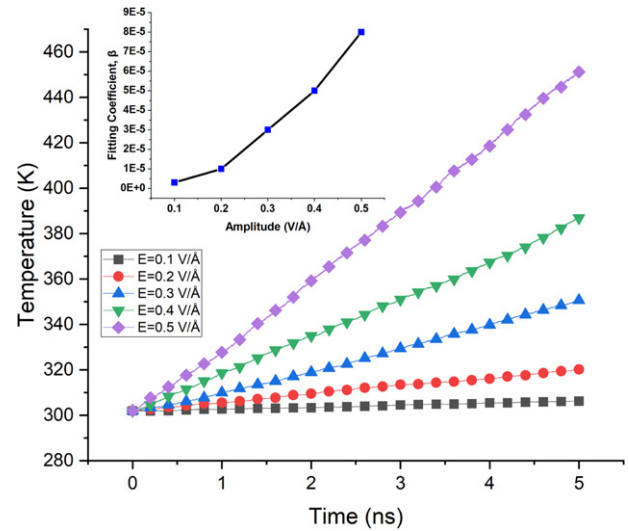

Figure 1. The time evolution of the temperature of a 3C-SiC pure bulk crystal under a 100 GHz MW radiation for the first 500 periods of the wave. The inset shows the heating rate represented by the fitting coefficient, β, for various electric field strengths.

moment in the SiC substrate. The total potential energy of the system is given by:

$$V = \sum_{i<j} V_{ij}^{(2)}\left(r_{ij}\right) + \sum_{ij<k} V_{jik}^{(3)}\left(r_{ij}, r_{ik}\right), \qquad (1)$$

where V is the effective interatomic interaction potential, $V_{jik}^{(3)}\left(r_{ij}, r_{ik}\right)$ represents the three-body interaction potential. The two-body interaction potential is given by,

$$V_{ij}^{(2)}\left(r\right) = \frac{H_{ij}}{r^{\eta_{ij}}} + \frac{Z_i Z_j}{r} e^{-r/\lambda} - \frac{D_{ij}}{2r^4} e^{-r/\xi} - \frac{W_{ij}}{r^6}, \qquad (2)$$

where H_{ij} represents the steric repulsion between the ith and jth atoms, D_{ij} is the strength of the charge-dipole attraction, W_{ij} is the strength of Van der Waals interaction, and $\frac{Z_i Z_j}{r} e^{-r/\lambda}$ is the Coulomb interaction term. More details on the expressions can be found in the original work of Vashishta *et al* (23).

The bulk SiC was simulated using a 4096-atom supercell of the cubic zinc-blende structure (3C-SiC) obtained by replicating the unit cell $8 \times 8 \times 8$ times along the three crystallographic axes, with periodic boundaries. The supercell size and structure were chosen following the published work on modelling interaction potential for SiC systems in Vashishta *et al* (23). The cubic cell size was 34.784 Å on each side, and the density was 3.2175 g/cc for the bulk. For surface calculations, $5 \times 5 \times 20$ supercell having 4100 atoms was used instead, with a 4.345 nm vacuum on top and bottom along the *z*-direction, which is the [001] crystal direction. The slab contains a silicon-terminating surface on top and a carbon-terminating surface at the bottom, keeping the total number of carbon and silicon equal (2050 carbon and 2050 silicon). The simulated SiC slab was anchored to the centre of mass of the system.

All simulations were first equilibrated at 300 K using the constant pressure and temperature (NPT) ensemble for 25 ps, followed by a microcanonical (NVE) run with an alternating
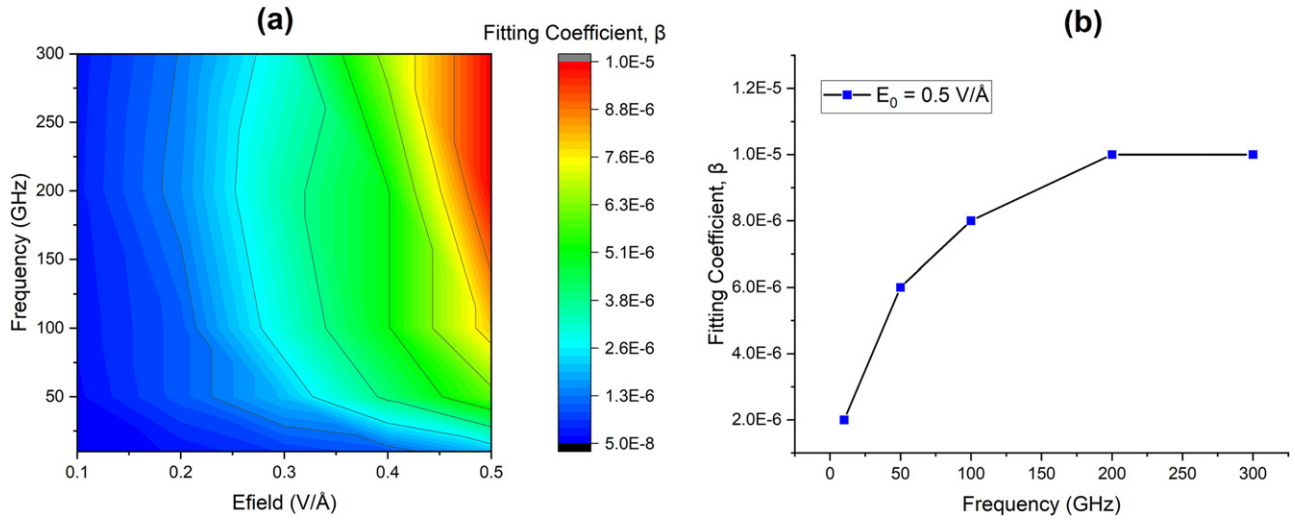
Figure 2. (a) The 2D heat map showing the impact of electric field intensity and frequency on the fitting coefficient (heating rate) of pure bulk 3C-SiC crystal. (b) β vs Frequency when the amplitude is kept constant at 0.5 V Å^{-1}.

Table 1. The values for cumulative Gaussian function for β.

$$\beta = A + 0.25B \left(1 + \text{erf}\left(\frac{E_{\text{field}}\left(\text{V Å}^{-1}\right) - C}{\sqrt{2}D}\right)\right) \left(1 + \text{erf}\left(\frac{\text{Frequency(GHz)} - \text{'}E}{\sqrt{2}F}\right)\right)$$

Fitting parameters	Values
A	$-2.3767 \times 10^{-7} \pm 3.5054 \times 10^{-7}$
B	$2.805\,87 \times 10^{-5} \pm 2.026\,19 \times 10^{-5}$
C	$0.593\,85 \pm 0.198\,25$
D	$0.252\,29 \pm 0.085\,62$
E	$39.889\,57 \pm 4.948\,74$
F	$47.544\,87 \pm 6.175\,73$

electric field to mimic microwave field, following the previous microwave heating studies modelled in LAMMPS by Afify and Sweatman (1) and Wang *et al* (24). The timestep was taken as 1 fs, and the periodic boundary conditions were chosen for the systems. Since SiC is a non-magnetic material, microwave interaction is dominated by the electric field. The oscillating electric field is introduced according to the following equation:

$$\boldsymbol{E}(t) = \boldsymbol{e_n} E_0 \, \sin\left(2\pi f t\right), \qquad (3)$$

where, E_0 is the amplitude, $\boldsymbol{e_n}$ is the direction of the electric field, f is the frequency, and t is the elapsed time of the MW radiation. The MW–material interaction is introduced by adding a force $\boldsymbol{F}_i(t) = q_i \boldsymbol{E}(t)$ to each atom i in the system, where q is the charge of the atom. For this system, charges assigned were Si $= 1.201$ and C $= -1.201$ electron charge unit according to Vashishta *et al* (23). In this study, the MW field was applied in the [100] direction for the bulk crystal and in the [100] and [001] directions for the slab. This model was tested with Vashishta potential on a (001) surface orientation slab under conventional heating and found similar melting temperature. Vashishta *et al* (23) reported the melting point of bulk SiC to be around 3200 K and the current system of layer SiC started melting at around 2700 K and completely melted at

3100 K. Also the system was constrained by the center-of-mass position of the slab by adjusting the coordinates of the atoms every timestep. This ensured there was no oscillation in phase with the electric field. It is worth noting that MW radiation is 'emulated' in LAMMPS by directly applying a force on atoms, i.e., we assume perfect and direct energy transfer from electromagnetic to kinetic in these simulations.

3. Results and discussion

MW irradiation at 100 GHz frequency with various electric field intensities (from 0.1 to 0.5 V Å^{-1}) was applied to bulk SiC to demonstrate the heating. The heating profiles (temperature vs time) shown in figure 1 confirms the temperature dependence of the heating rates of SiC demonstrated in the previous studies by Tandon *et al* (22) and Zhang *et al* (2014). The heating profile was approximately fitted to an exponential growth equation of the form $T(t) = T_0 e^{\beta t}$, where T is the temperature in Kelvin (K), t is the elapsed simulation time in nanoseconds (ns), T_0 is the initial temperature of the system and β is the fitting coefficient which is considered to convey the heating rates of the material.

Understandably, the heating rate increases with the electric field intensity of the applied microwave due to the increase
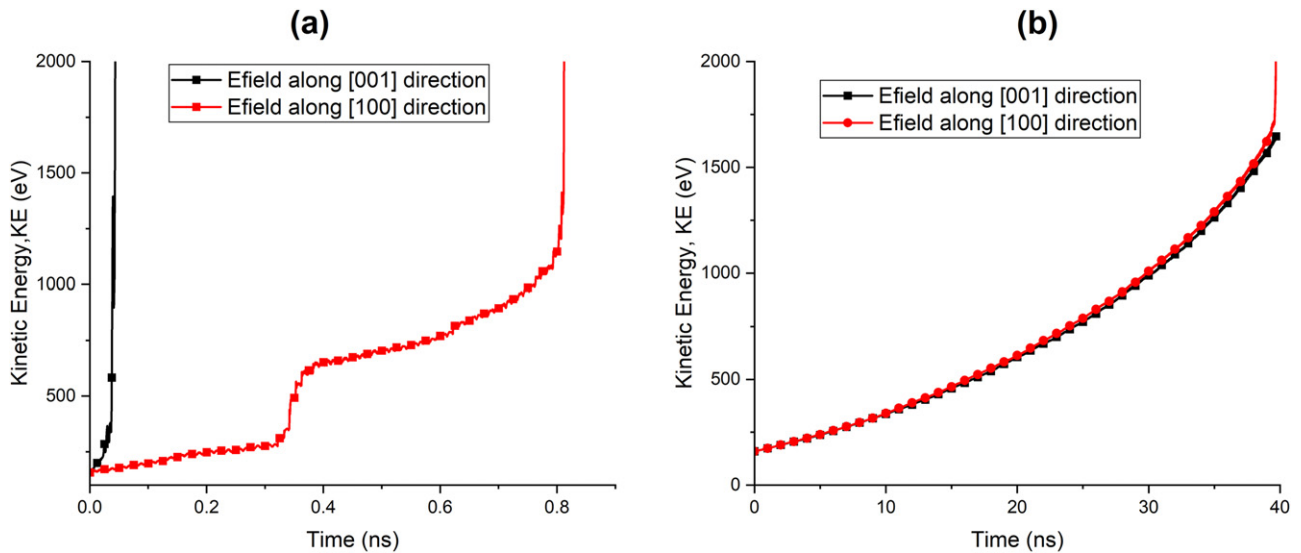
Figure 3. Time evolution of temperature of 3C-SiC (a) surface and (b) bulk when irradiated with 500 cycles of 100 GHz, 0.5 V A^{-1} microwave radiation along *z*-axis or [100] direction (red) and *x*-axis or [001] direction (black).
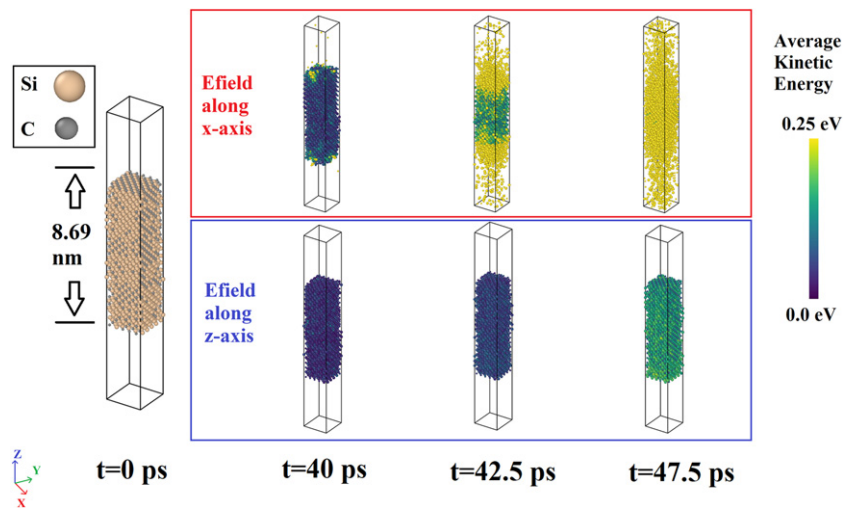

Figure 4. On the left, SiC slab with void on top and bottom along the *z*-axis. Snapshots in the top (*E*-field along the [001] direction or *x*-axis) and the bottom (*E*-field along the [100] direction *z*-axis) showing kinetic energies and the structural information at three different timesteps during the MW heating.

in the radiative input energy. The inset shows the impact of the electric field strength on the fitting coefficient β. A square-law relationship is observed between β and the electric field amplitude, which is expected for MW heating as showed for MW heating of water by Afify and Sweatman (1).

Microwave heating profiles for 3C-SiC for various frequencies were extracted for constant field intensities. A 2D heat map is shown in figure 2(a), which displays the heating profiles for microwave frequencies of 10, 50, 100, 200 and 300 GHz and amplitude from 0.1 to 0.5 for the first 500 MW radiation cycles. The fitting coefficients, β were obtained similarly for all heating profiles and were normalized for power. Figure 2(b) shows the heating rate and MW frequency relationship when the amplitude is constant at 0.5 V Å^{-1}.

Fitting of the heatmap contours revealed that the relationship is accurately described by a cumulative Gaussian function ($R^2 = 0.984$) rather than the expected exponential function ($R^2 = 0.62$). This supports the finding in the previous study of Tandon *et al* (22), where it was experimentally observed that the heating profile could not be described using a single exponential function. Table 1 shows the values of the fitting parameters A and B (unitless), E (in GHz), C is in the same units as D, $\dot{E}$ is in the same units as F. Also to note that 'E_{field}' represents the electric field (in Volts per Angstrom, V Å^{-1}) and 'frequency' (in GHz) of the applied MW.

Directional MW with the same frequency and power was applied to the surface structure crystal along the X and Z axes (equivalent to parallel and perpendicular directions to the surface, respectively). The resultant heating profiles are compared and shown in figure 3(a).

MW heating in the bulk crystal, shown in figure 3(b), demonstrates the same heating behaviour as in figure 1 with no discernable difference in heating between the two directional microwave radiations. However in the presence of a surface, the heating dynamics heavily depend on the direction of the applied microwave.

Figure 4 shows the structural evolution of the SiC slab during heating under MW radiations parallel and perpendicular to the surface. The time-averaged kinetic energy (for every 250 fs) visualization in figure 4 is taken for 100 GHz, 0.5 V A^{-1} microwave radiation along [001] and [100] to the layered SiC.

When MW radiation is applied in the [001] direction or *x*-axis, local melting and spallation occur near the surface, as shown in figure 4 in the snapshot at $t = 40$ ps. The system gradually melts at the top and bottom at $t = 42.5$ ps as more atoms are energized and finally completely melt after $t = 47.5$ ps. Figure 4 shows hotspots near the surface, which suggests that melting initiates near the surface. The process of surface atoms initiating to break away from the crystal can be compared to random crystal growth from a seed atom within a molten substrate as such that in both cases the process is quite random. At first few atoms from the surface gets superheated and escapes into the void, creating a sharp increase in the overall kinetic energy change. The heating rate of the temperature evolution vs time curve is seen to have a 'knee' formation in figure 3(a) around that timestep. The knee formation indicates the beginning of local melting at the surface and this is observed irrespective of the MW irradiation direction. This result agrees with the previous theoretical studies done by Hu *et al* (10) and Phillpot *et al* (19) and experimental study done by Newman (18). As for pure bulk SiC, 'mechanical melting' was observed, also demonstrated by Phillpot *et al* (19) in their paper. Mechanical melting is defined as a homogeneous crystal lattice breakdown (unlike thermodynamic melting, which arises around the crystal defects and surfaces) that transforms the crystal into the liquid phase within a few femtoseconds.

The bottom portion of figure 4 shows the snapshots of the system when MW is applied perpendicular ([100] direction) to the surface, which shows little to no heating compared to the corresponding parallel MW heating. The directional heating of the layered SiC system suggests that the system will melt much quicker (~20 times faster) when the MW radiation is incident parallel to the surface of the void. This phenomenon may be attributed to the nature of the surface bonds. The dangling bonds at the surface produce orientation-dependent polarization which seems to play a deciding role in the higher MW heating rate in the *x*-direction. Further studies on different surface orientations and terminations may reveal the impact of the surface effects on microwave heating.

4. Conclusion

MW heating of 3C-SiC crystal was studied using MD simulations. The heating rate for the bulk SiC unilaterally increases with increasing electric field intensity, and the dependence of heating rate on the electric field and frequency shows a cumulative Gaussian behaviour and not the expected exponential behaviour. The heating profile of the defect-free bulk SiC shows no dependence on the direction of the MW radiation, whereas SiC slabs with surfaces along [100] direction show that the heating profile is direction-dependent. MW radiation applied parallel to the SiC surface caused the crystal to melt approximately nineteen times faster than MW radiation perpendicular to the surface.

Author contributions

Tahsin Ashraf Khan: investigation, methodology, writing—original draft. **Binesh Puthen Veettil**: resources, methodology, writing, review & editing. **Patrick Burr**: conceptualization, methodology, validation, review & editing. **David Payne**: methodology, review & editing. **Mattias Juhl**: methodology, review & editing. **Utshash Das**: review & editing. **Brett Hallam**: review & editing. **Darren Bagnall**: review & editing.

Conflict of interest

The authors declare that they have no known competing financial interests or personal relationships that could have appeared to influence the work reported in this paper.

Data availability

The data that support the findings of this study are available from the corresponding author upon reasonable request.

ORCID iDs

Tahsin Ashraf Khan ⬚ https://orcid.org/0000-0002-2665-3427
Patrick A Burr ⬚ https://orcid.org/0000-0003-4796-9110

References

[1] Afify N D and Sweatman M B 2018 Classical molecular dynamics simulation of microwave heating of liquids: the case of water *J. Chem. Phys.* **148** 024508
[2] Alford T L, Thompson D C, Mayer J W and Theodore N D 2009 Dopant activation in ion implanted silicon by microwave annealing *J. Appl. Phys.* **106** 114902
[3] Brooks C L III, Case D A, Plimpton S, Roux B, van der Spoel D and Tajkhorshid E 2021 Classical molecular dynamics *J. Chem. Phys.* **154** 100401
[4] Cao M-S, Wang X-X, Cao W-Q and Yuan J 2015 Ultrathin graphene: electrical properties and highly efficient electromagnetic interference shielding *J. Mater. Chem.* C **3** 6589–99

[5] Cao M-S, Song W-L, Hou Z-L, Wen B and Yuan J 2010 The effects of temperature and frequency on the dielectric properties, electromagnetic interference shielding and microwave-absorption of short carbon fiber/silica composites *Carbon* **48** 788–96

[6] Deng X *et al* 2020 Investigation and failure mode of asymmetric and double trench SiC mosfets under avalanche conditions *IEEE Trans. Power Electron.* **35** 8524–31

[7] El Khaled D, Novas N, Gazquez J A and Manzano-Agugliaro F 2018 Microwave dielectric heating: applications on metals processing *Renew. Sustain. Energy Rev.* **82** 2880–92

[8] García-Baños B, Reinosa J J, Peñaranda-Foix F L, Fernández J F and Catalá-Civera J M 2019 Temperature assessment of microwave-enhanced heating processes *Sci. Rep.* **91** 1–10

[9] Gong P, Yang Y-Y, Ma W-D, Fang X-Y, Jing X-L, Jia Y-H and Cao M-S 2021 Transport and recombination properties of group-III doped SiCNTs *Physica* E **128** 114578

[10] Hu Y, Nakano A and Wang J 2017 Directional melting of alumina via polarized microwave heating *Appl. Phys. Lett.* **110** 044102

[11] Ibrahim M, Rahim R A, Nordin J M, Zulaika S, Nyzam A and Amira N 2019 Dielectric properties characterization of the rice and rice weevil for microwave heating treatment *Indones. J. Electr. Eng. Comput. Sci.* **13** 752–8

[12] Isfort P, Penzkofer T, Pfaff E, Bruners P, Gü R W, Schmitz-Rode T and Mahnken A H 2010 Silicon carbide as a heat-enhancing agent in microwave ablation: *in vitro* experiments *CardioVascul. Intervent. Radiol.* **34** 833

[13] Jia Y-H, Gong P, Li S-L, Ma W-D, Fang X-Y, Yang Y-Y and Cao M-S 2020 Effects of hydroxyl groups and hydrogen passivation on the structure, electrical and optical properties of silicon carbide nanowires *Phys. Lett.* A **384** 126106

[14] Jiang W, Sun M, Zhang K, Dai X, Xia Y, Wang D, Xie A and Wu F 2016 Using γ-Fe_2O_3 to tune the electromagnetic properties of three-dimensional (3D) polypyrrole (PPy) and its broadband electromagnetic absorber *RSC Adv.* **6** 68128–33

[15] Kremsner J M and Kappe C O 2006 Silicon carbide passive heating elements in microwave-assisted organic synthesis *J. Org. Chem.* **71** 4651–8

[16] Liang C, Liu C, Wang H, Wu L, Jiang Z, Xu Y, Shen B and Wang Z 2014 SiC-Fe_3O_4 dielectric-magnetic hybrid nanowires: controllable fabrication, characterization and electromagnetic wave absorption *J. Mater. Chem.* A **2** 16397–402

[17] Nelson B W, Lemmon A N, DeBoi B T, Hossain M M, Mantooth H A, New C D and Helton J C 2020 Computational efficiency analysis of SiC MOSFET models in SPICE: static behavior *IEEE Open J. Power Electron.* **1** 499–512

[18] Newman R C 1982 Defects in silicon *Rep. Prog. Phys.* **45** 1163–210

[19] Phillpot S R, Yip S and Wolf D 1998 How do crystals melt? *Comput. Phys.* **3** 20

[20] Sarswat P K and Free M L 2013 An investigation of rapidly synthesized Cu_2ZnSnS_4 nanocrystals *J. Cryst. Growth* **372** 87–94

[21] Singh S, Gupta D, Jain V and Sharma A K 2015 Microwave processing of materials and applications in manufacturing industries: a review *Mater. Manuf. Process.* **30** 1–29

[22] Tandon R, Wereszczak A and Lara-Curzio E 2006 Heating rates of silicon carbide in a microwave field *Mech. Prop. Perform. Eng. Ceram. Compos. II* **27**

[23] Vashishta P, Kalia R K, Nakano A and Rino J P 2007 Interaction potential for silicon carbide: a molecular dynamics study of elastic constants and vibrational density of states for crystalline and amorphous silicon carbide *J. Appl. Phys.* **101** 103515

[24] Wang C, Liu H, Song L, Tan J, Yang W and Cheng L 2021 Temperature evolution, atomistic hot-spot effects and thermal runaway during microwave heating of polyacrylonitrile: a ReaxFF molecular dynamics simulation *Nano Sel.* **2** 2373

[25] Wang H, Wu L, Jiao J, Zhou J, Xu Y, Zhang H, Jiang Z, Shen B and Wang Z 2015 Covalent interaction enhanced electromagnetic wave absorption in SiC/Co hybrid nanowires *J. Mater. Chem.* A **3** 6517–25

[26] WanJun Y, TingHong G, XiaoTian G, YunXiang Q and Quan X 2013 SCIENCE china physics, mechanics & astronomy melting kinetics of bulk SiC using molecular dynamics simulation *Sci. China. Phys. Mech. Astron.* **56** 1699–704

[27] Yang H, Cao M, Li Y, Shi H, Hou Z, Fang X, Jin H, Wang W and Yuan J 2014 Enhanced dielectric properties and excellent microwave absorption of SiC powders driven with NiO nanorings *Adv. Opt. Mater.* **2** 214–9

[28] Yang M, Zhou W, Liu Y, Li L, Luo F and Zhu D 2019 $LiCo_xNi_{1-x}O_2$ with high dielectric and microwave absorption performance in X-band *Ceram. Int.* **45** 17800–5

[29] Zhang M, Cao M-S, Shu J-C, Cao W-Q, Li L and Yuan J 2021 Electromagnetic absorber converting radiation for multifunction *Mater. Sci. Eng.* R **145** 100627

[30] Thompson A P *et al* 2022 LAMMPS - a flexible simulation tool for particle-based materials modeling at the atomic, meso, and continuum scales *Comput. Phys. Commun.* **271** 108171

[31] Zhang Y, Li J-L, Wang X Y, Wang J P and Wang B Z 2014 Molecular dynamics simulation on temperature and structure characteristics of microwave-heating NaCl solution *MMWCST 2013-Proc. 2013 Int. Work. Microw. Millim. Wave Circuits Syst. Technol* pp 161–4